Available online at www.sciencedirect.com
SCIENCE DIRECT®

Fluid Phase Equilibria 219 (2004) 181–193

FLUID PHASE EQUILIBRIA

www.elsevier.com/locate/fluid

# Vapor-phase chemical equilibrium for the hydrogenation of benzene to cyclohexane from reaction-ensemble molecular simulation

Javier Carrero-Mantilla, Mario Llano-Restrepo*

*School of Chemical Engineering, Universidad del Valle, Apartado 25360, Cali, Colombia*

Received 2 October 2003; received in revised form 18 February 2004; accepted 25 February 2004

---

**Abstract**

The reaction-ensemble Monte-Carlo (REMC) molecular simulation method was used to study the vapor-phase chemical equilibrium for the reaction of hydrogenation of benzene to cyclohexane. A one-center modified Buckingham exponential-6 (1CMBE6) effective pair potential model (that had already been used to predict thermodynamic properties and liquid–liquid equilibria of helium + hydrogen mixtures) was used for hydrogen. Six-center modified Buckingham exponential-6 (6CMBE6) effective pair potential models (that had already been used to reproduce the saturated liquid and vapor densities, vapor pressures, second virial coefficients, and critical parameters of the six-membered ring molecules), were used for benzene and cyclohexane. No binary adjustable parameters were needed to compute the unlike-pair Buckingham exponential-6 interactions in the ternary system. Simulation results were obtained for the effect of some operating variables such as temperature (from 500 to 650 K), pressure (from 1 to 30 bar), and hydrogen to benzene feed mole ratio (from 1.5:1 to 6:1) on the reaction conversion, molar composition, and mass density of the ternary system at equilibrium. These results were found to be in excellent agreement with calculations using the predictive Soave–Redlich–Kwong (PSRK) group contribution equation of state.

*Keywords:* Chemical equilibrium; Reaction ensemble; Molecular simulation; Benzene; Hydrogen; Cyclohexane

---

## 1. Introduction

In the petrochemical industry, cyclohexane ($C_6H_{12}$) is mainly produced from the hydrogenation of benzene ($C_6H_6$), according to the reaction:

$$C_6H_6 + 3H_2 \leftrightarrow C_6H_{12}$$

for which a hydrogen to benzene mole ratio of 3:1 is stoichiometrically required. Cyclohexane can also be recovered directly from natural gasoline and petroleum naphta [1]. However, the dehydrogenation of cyclohexane and its derivatives (present in naphtas) to aromatic hydrocarbons is an important reaction in the catalytic reforming process used in refinery to produce high octane motor fuels [2–4]. From petroleum fractions, it is difficult to obtain the very high quality cyclohexane product achieved by benzene hydrogenation [5–7]. Most of cyclohexane is oxidized to cyclohexanol and cyclohexanone for making caprolactam and adipic acid, which in turn are used as precursors of nylon 6 and nylon 6/6, respectively [1,5,6]. A small amount of cyclohexane is used as a solvent for cellulose ethers, high-density polyethylene, rubber, fats and essential oils, and as a varnish and paint remover.

Older methods of benzene hydrogenation use a mixed (vapor and liquid) phase process while newer methods use a vapor-phase process [1,7]. In mixed-phase processes [8–11], a portion of the liquid cyclohexane product is recycled to the reactors to remove the exothermic heat of reaction by vaporization of the liquid phase. Due to the presence of cyclohexane in the feed, two, three or four reactors in series are typically used to complete the hydrogenation reaction using nickel or a noble metal (like platinum or palladium) as catalysts supported on alumina or silica. Benzene is fed in parallel flow into each of the reactors while hydrogen and recycle cyclohexane are passed through in series flow from the first to the last reactor. In contrast, in vapor-phase processes [12–18], a single reactor suffice to complete the hydrogenation reaction because the need to recycle cyclohexane is eliminated by the use of steam generation to remove the heat of reaction. The vapor-phase hydrogenation

---

* Corresponding author. Tel.: +57-2-3312935; fax: +57-2-3392335.
*E-mail address:* mllano@mafalda.univalle.edu.co (M. Llano-Restrepo).

0378-3812/$ – see front matter © 2004 Elsevier B.V. All rights reserved.
doi:10.1016/j.fluid.2004.02.009

of benzene to cyclohexane is carried out catalytically in a tubular reactor, using noble metals as catalysts specifically formulated to inhibit completely the side reaction in which cyclohexane is isomerized to methylcyclopentane. Catalyst is packed in the tubes, and boiler feed water is circulated in the shell for the removal of reaction heat via steam generation. Fresh benzene is combined with makeup and recycle hydrogen and preheated before entering the reactor. A stoichiometric value of 3:1 for the hydrogen to benzene (H:B) feed mole ratio is typically used [17]. However, the H:B feed mole ratio may be 5:1 [12], 8:1 or greater with an upper limit of 25:1 [15]. For low purity feed hydrogen, the higher values of the H:B feed mole ratio are favored. Reactor pressures are in the range 10–35 bar [1,6,12]. Reaction temperatures are in the range 450–670 K [1,6,12,15,18]. Use of high temperatures increases the reaction rate. However, since the reaction is highly exothermic [1,6], its equilibrium conversion decreases at higher temperatures, and the reaction is then limited by chemical equilibrium. As a result, the temperature of the reactor should be set as a compromise between kinetics and thermodynamics. It is therefore of the utmost importance to study the effect of some operating variables such as temperature, pressure, and H:B feed mole ratio on the chemical equilibrium of this reaction.

The effect of H:B feed mole ratio and reactor pressure on the chemical equilibrium of the vapor-phase hydrogenation of benzene to cyclohexane has been studied by Abraham and Chapman [7]. To calculate the equilibrium conversion, ideal gas behavior was assumed for the three species involved in the reaction. A computer program was developed and presented by those authors to calculate the benzene content in the cyclohexane product at equilibrium conditions. Results were reported for three temperature values: 505, 561, and 616 K, three pressure values: 32, 36, and 39 bar, three H:B feed mole ratio values: 8:1, 16:1, and 24:1, and three feed hydrogen purity values: 75, 85, and 100 vol.%. As expected from a consideration of Le Châtelier's principle, it was shown by those authors that a decrease in temperature, an increase in pressure, an increase in the H:B feed mole ratio, and an increase in feed hydrogen purity, decrease the benzene content of cyclohexane product by increasing the conversion of benzene to cyclohexane.

Since a reliable and economic design of a vapor-phase tubular reactor depends on accurate estimates of volumetric properties (like compressibility factor or density) of the mixture of reactants and products, which in turn, depend on the molar composition of the mixture, it would be of interest to ascertain the validity of the ideal gas behavior assumption made by Abraham and Chapman [7] to compute the molar composition at equilibrium in the benzene hydrogenation vapor-phase reactor. To consider the nonideality of the vapor phase, an equation of state could in principle be used to compute the partial fugacity coefficients of benzene, hydrogen, and cyclohexane in the ternary mixture as a function of temperature, pressure, and composition, as required for the calculation of the extent of reaction at equilibrium. However, application of any of the most popular equations of state to mixtures requires the values of the binary interaction parameters that are involved in the mixing rules used to compute the equation of state parameters of the mixture. For the interaction of hydrogen with other compounds, it happens that the values of those parameters are not easily accessible; in fact, they are usually found to be hidden or "hard-wired" into the parameter databases of current commercial process simulators (see, for instance, ref. [19]).

In consequence, predictive methods that do not need any binary interaction parameters turn out to be a convenient choice if the nonideality of the vapor-phase is taken into consideration for the computation of the chemical equilibrium of the hydrogenation of benzene to cyclohexane. The predictive Soave–Redlich–Kwong (SRK) group-contribution equation of state (known as PSRK method), which was devised and developed by Gmehling and co-workers [20–25], combines the SRK equation of state [26] with the original UNIFAC group contribution method [27–32], and does not require any binary interaction parameters for the mixing rules that are used to compute the mixture parameters. The PSRK method has shown to be very successful for the prediction of gas solubilities and vapor–liquid equilibria at low and high pressures, even for highly asymmetric systems [20–25]. This method is based on the original (or revised, if necessary) UNIFAC structural groups and corresponding group interaction parameters, whose values were found by fitting vapor–liquid equilibria at low pressure [27–32]. However, for the development of the PSRK method, the UNIFAC database has been extended to gases at supercritical conditions by fitting gas solubilities and vapor–liquid equilibria at high pressure. These gases have been added as new structural groups to the list of groups already existing in UNIFAC. In that way, $H_2$ is a group by itself whose interaction parameters with other groups in the database were found by fitting available VLE and gas solubility data for hydrogen-containing systems. This makes it possible to use the PSRK method for the estimation of partial fugacity coefficients in the ternary system of benzene, hydrogen, and cyclohexane and the computation of its chemical equilibrium. Because the required group interaction parameters were found by fitting solubilities and VLE experimental data of some of the binary subsystems, results obtained for the chemical equilibrium of the ternary system would indeed be predictive.

Although molecular simulation calculations may sometimes make use of binary interaction parameters into the combining rules that are used to compute the potential parameters of the unlike-pair interactions, it has been shown, in some cases [33–35], that it is possible to ignore the binary interaction parameters and still obtain very good results for mixture phase behavior. Such a successful prediction of mixture properties by the sole use of pure component properties is a severe test for the predictive capability of current intermolecular potential models.

The reaction-ensemble Monte–Carlo (REMC) method devised by Smith and Triska [36] has been applied successfully by Lisal et al. [37,38] to the calculation of chemical and phase equilibria of binary and ternary systems without using binary interaction parameters to compute the unlike-pair interactions. This method can be applied to the prediction of the chemical equilibrium of the hydrogenation of benzene to cyclohexane if suitable intermolecular potential models are found and implemented for the three species involved in the reacting system. In that direction, a one-center modified Buckingham exponential-6 (1CMBE6) effective pair potential model for hydrogen that was successfully used by Liu and Beck [39] to predict thermodynamic properties and liquid–liquid equilibria of helium + hydrogen mixtures at 300 K and 54 kbar, may be tested for the computation of the chemical equilibrium of interest to this work. Also, six-center modified Buckingham exponential-6 (6CMBE6) effective pair potential models for benzene and cyclohexane that were developed by Errington and Panagiotopoulos [40], may be tested for the same purpose. These latter potential models were optimized by their proponents in an attempt to reproduce as accurately as possible the saturated liquid and vapor densities, vapor pressures, second virial coefficients, and critical parameters of the six-membered ring molecules.

Because the development and testing of potential models that remain valid over wide ranges of state conditions and for a variety of systems of practical significance has been identified as one of the most important tasks for the continuing application of molecular simulation methods to the prediction of phase and chemical equilibria [41], it would be of interest to find out whether the above mentioned potential models for hydrogen, benzene, and cyclohexane are capable of predicting the chemical equilibrium of this ternary system.

Since the 6CMBE6 potential models were fitted to reproduce saturated liquid and vapor properties, their use for the computation of chemical equilibrium in the vapor-phase, far away from saturation, is an extrapolation of predictive nature, whose validity, in absence of experimental data, should be judged indirectly from a comparison with results obtained from an entirely different predictive approach, such as the PSRK method mentioned above.

In consequence, the aim of this work is to assess the effect of temperature, pressure, and H:B feed mole ratio on the chemical equilibrium of the nonideal vapor-phase hydrogenation of benzene to cyclohexane by use of both the REMC and the PSRK methods, and to test (at least indirectly, due to the lack of experimental chemical equilibrium data) the predictive capabilities of the effective pair potential models used for the three species involved in the reaction, from a comparison between the molecular simulation and the equation of state results. In Section 2, details are given for the potential models used to describe the molecular interactions of the pure substances and the ternary system considered in this study. In Section 3, important molecular simulation details are provided for the purpose of making the results of this work as reproducible as possible. In Section 4, details are given for the computation of the chemical equilibrium from classical thermodynamics and the PSRK method. In Section 5, REMC molecular simulation results are reported and compared with results obtained from the PSRK method and also from the ideal gas behavior assumption.

## 2. Intermolecular potential models

In the present work, hydrogen is described as a 1CMBE6 fluid, and benzene and cyclohexane as 6CMBE6 fluids. The 1CMBE6 potential model used by Liu and Beck [39] to predict thermodynamic properties and liquid–liquid equilibria of helium + hydrogen mixtures, is chosen for hydrogen. 6CMBE6 potential models were used by Errington and Panagiotopoulos [40] to model the nonbonded interactions between groups on different molecules of benzene or cyclohexane. Even though bond-bending and torsional intramolecular contributions were also taken into account by those authors for the development of their potential models for benzene and cyclohexane, the distributions of bending and dihedral angles turned out to be peaked at the values corresponding to a rigid (nonflexible) geometry (planar for benzene and the chair conformation for cyclohexane). In consequence, the parameters of the 6CMBE6 potential models were optimized by those authors to reproduce, as accurately as possible, the saturated liquid and vapor densities, vapor pressures, second virial coefficients, and critical parameters of the six-membered ring molecules.

These molecular models are used to compute the total configurational energy $U$ of these fluids by use of the pairwise additivity approximation with effective pair potentials $\phi_{ij}$ given by the sum of modified Buckingham exponential-6 (MBE6) interactions $\phi_{kl}^{\mathrm{MBE6}}$ between all pairs of intermolecular sites $k$ (in molecule $i$) and $l$ (in molecule $j$):

$$U = \sum_i \sum_j \phi_{ij} \tag{1}$$

where

$$\phi_{ij} = \sum_{k\in i} \sum_{l\in j} \phi_{kl}^{\mathrm{MBE6}} \tag{2}$$

The MBE6 potential of interaction is given by the expression [42,43]:

$$\phi^{\mathrm{MBE6}}(r) = \begin{cases} \dfrac{\varepsilon}{1-(6/\alpha)}\left[\dfrac{6}{\alpha}\exp\left(\alpha\left[1-\dfrac{r}{r_{\mathrm{m}}}\right]\right)-\left(\dfrac{r_{\mathrm{m}}}{r}\right)^{6}\right], & \text{for } r > r_{\max} \\ \infty, & \text{for } r < r_{\max} \end{cases} \tag{3}$$

The potential function for $r > r_{\text{max}}$ is the original Buckingham exponential-6 (BE6) potential model, which exhibits a spurious maximum at a radial distance $r = r_{\text{max}}$. Because of the occurrence of this maximum and due to the fact that the potential becomes infinitely negative (instead of infinitely positive) at $r = 0$, the original BE6 potential is modified by making it infinitely repulsive (instead of largely attractive) for all separations closer to $r_{\text{max}}$, which is known as the inner cutoff distance.

In Eq. (3), $\varepsilon$, $\alpha$, and $r_{\text{m}}$ are the three parameters of the MBE6 potential with $r_{\text{m}}$ as the radial distance at which the original BE6 potential reaches a minimum value of $-\varepsilon$. The inner cutoff distance $r_{\text{max}}$ corresponds to the smallest root of the following transcendental equation that arises from applying the necessary condition $\mathrm{d}\phi^{\text{BE6}}(r)/\mathrm{d}r = 0$ to the original BE6 potential [42]:

$$\left(\frac{r_{\text{max}}}{r_{\text{m}}}\right)^7 \exp\left(\alpha\left[1-\frac{r_{\text{max}}}{r_{\text{m}}}\right]\right) - 1 = 0 \tag{4}$$

Sometimes, instead of the parameter $r_{\text{m}}$ an alternative size parameter $\sigma$ is used, which is defined as the radial distance at which the original BE6 potential is zero. Thus, once the parameter $\alpha$ has been set, the parameters $\sigma$ and $r_{\text{m}}$ can be related through the following equation:

$$\frac{6}{\alpha}\exp\left(\alpha\left[1-\frac{\sigma}{r_{\text{m}}}\right]\right) - \left(\frac{r_{\text{m}}}{\sigma}\right)^6 = 0 \tag{5}$$

The size and energy parameters $\sigma_{kl}$ and $\varepsilon_{kl}$ for the site $k$-site $l$ interaction can be defined in terms of the size and energy parameters $\sigma_k$, $\sigma_l$ and $\varepsilon_k$, $\varepsilon_l$ of the molecules that lodge the sites by the commonly used combining rules:

$$\sigma_{kl} = \frac{\eta}{2}(\sigma_k + \sigma_l) \tag{6}$$

$$\varepsilon_{kl} = \zeta(\varepsilon_k \varepsilon_l)^{1/2} \tag{7}$$

where $\eta$ and $\zeta$ are adjustable coefficients (known as binary interaction parameters).

If $\eta = \zeta = 1$, Eqs. (6) and (7) simplify to the well-known Lorentz–Berthelot combining rules [44]:

$$\sigma_{kl} = \tfrac{1}{2}(\sigma_k + \sigma_l) \tag{8}$$

$$\varepsilon_{kl} = (\varepsilon_k \varepsilon_l)^{1/2} \tag{9}$$

The steepness parameter $\alpha_{kl}$ for the site $k$-site $l$ interaction can be defined in terms of the steepness parameters $\alpha_k$ and $\alpha_l$ of the molecules that lodge the sites by a geometric mean combining rule [40]:

$$\alpha_{kl} = (\alpha_k \alpha_l)^{1/2} \tag{10}$$

Due precisely to the fact that one of the aims of this work is to ascertain the ability of the MBE6 potential models for hydrogen, benzene, and cyclohexane to predict the effect of the temperature, pressure, and hydrogen to benzene feed mole ratio on the chemical equilibrium of the ternary system, then no binary interaction parameters should be involved in the calculations, and in consequence, the Lorentz–Berthelot combining rules, Eqs. (8) and (9), together with Eq. (10), are employed to compute the unlike-pair site–site MBE6 interactions.

Table 1
Parameters for the site-site interactions with the potential models used in this work

| Interaction | $\sigma$ (Å) | $\varepsilon/k$ (K) | $\alpha$ | $r_{\text{m}}$ (Å) | $r_{\text{max}}$ (Å) |
|---|---|---|---|---|---|
| BB | 3.710 | 74.06 | 20 | 4.067 | 0.285 |
| CC | 3.910 | 77.40 | 20 | 4.286 | 0.301 |
| HH | 2.978 | 36.40 | 11.1 | 3.430 | 1.255 |
| BC | 3.810 | 75.71 | 20 | 4.176 | 0.293 |
| BH | 3.344 | 51.92 | 14.9 | 3.742 | 0.641 |
| CH | 3.444 | 53.08 | 14.9 | 3.854 | 0.661 |

Table 1 lists the values for the size, energy, and steepness parameters $\sigma$, $\varepsilon$, and $\alpha$, respectively, and the subsidiary parameters $r_{\text{m}}$ and $r_{\text{max}}$ for the six kinds of site $k$-site $l$ interactions in the ternary system of benzene (B), cyclohexane (C), and hydrogen (H).

For hydrogen, Liu and Beck [39] reported $r_{\text{m}}$ directly so that the corresponding value of $\sigma$ was found by solving Eq. (5) with $\alpha = 11.1$. In contrast, for benzene and cyclohexane, Errington and Panagiotopoulos [40] reported the size parameter $\sigma$ so that the corresponding value of $r_{\text{m}}$ was found by solving Eq. (5) with $\alpha = 20$. Values of $\sigma$, $\varepsilon$, and $\alpha$ for the unlike-pair site–site interactions were found from the combining rules given in Eqs. (8)–(10), and the corresponding values of $r_{\text{max}}$ were found by solving Eq. (4). Values of $r_{\text{m}}$ for the unlike-pair site–site interactions were found by solving Eq. (5).

## 3. Molecular simulation method

Since benzene and cyclohexane are described by six-site (i.e., united-atom) molecular models in this work, then it is necessary to define the site coordinates in a local molecular frame (the so-called internal coordinates). For benzene, a fixed planar geometry is assumed with a bond length equal to 1.40 Å and a bond bending angle of 120°. With one of the sites located at the origin, the Cartesian coordinates of all the other sites can be easily found by use of planar trigonometry. The resulting values of the internal coordinates of the six sites of the benzene molecules are given in Table 2.

Table 2
Internal cartesian coordinates $x$, $y$, $z$ (in Å) for the six sites of the benzene molecules, with site $C_1$ located at the origin and the other sites located at the vertices of a regular hexagon and numbered counter-clockwise

| Site | $x$ | $y$ | $z$ |
|---|---|---|---|
| $C_1$ | 0 | 0 | 0 |
| $C_2$ | 1.400 | 0 | 0 |
| $C_3$ | 2.100 | 1.212 | 0 |
| $C_4$ | 1.400 | 2.425 | 0 |
| $C_5$ | 0 | 2.425 | 0 |
| $C_6$ | −0.700 | 1.212 | 0 |

For cyclohexane, a rigid non-planar geometry, corresponding to the chair conformation, is assumed. Among the four possible conformations of cyclohexane, namely, chair, semichair, boat, and twisted boat, the chair is the most stable one due to the absence of any bending and dihedral angle strains [45]. Actually, the chair and the twisted boat conformations (known as conformers) correspond to local minima in the potential energy surface whereas the semichair and the boat conformations correspond to local maxima. In consequence, the chair and the twisted boat conformations coexist at equilibrium at any temperature. However, due to the relatively large value of 23 kJ/mol [45] for the energy barrier between the two local minima, the distribution of conformers is strongly biased towards the chair conformation. Indeed, even at the highest temperature (650 K) considered in the present work, use of the Boltzmann distribution shows that 98.6% of the cyclohexane molecules exhibit the chair conformation.

In this work, the *z-matrix* approach [46], explained in geometrical terms by Essén and Svensson [47], is used to define the internal coordinates of the sites of the cyclohexane molecules in the chair conformation. Assuming that three sites $k$, $j$, $i$ have already been defined, in that order, the $z$-matrix specifies the relative position $\boldsymbol{r}_n$ of site $n$ (next in the sequence), by means of three geometric parameters: the distance $r(n, i)$ to neighboring site $i$, the bond angle $\theta(n, i, j)$ at site $i$ between lines $i$–$n$ and $i$–$j$, and the dihedral angle $\phi(n, i, j, k)$ between the two planes defined by $n$–$i$–$j$ and $i$–$j$–$k$. The bond angle is in the range $0 \leq \theta \leq 180°$, and the dihedral angle is in the range $-180° \leq \phi \leq 180°$. The $z$-matrix corresponding to the chair conformation of cyclohexane is given in Table 3.

Because the values of the distance $r(n, i)$, and the angles $\theta(n, i, j)$, and $\phi(n, i, j, k)$ are given in the $z$-matrix, it is possible to compute the position vector $\boldsymbol{r}_n$ from the following analytical formula given by Essén and Svensson [47]:

$$\begin{aligned}\boldsymbol{r}_n &= \boldsymbol{r}_i + r(n, i)\{\cos\theta(n, i, j)\boldsymbol{b}_{ij} \\ &\quad + \sin\theta(n, i, j)[\cos\phi(n, i, j, k)(\boldsymbol{b}_{ijk} \times \boldsymbol{b}_{ij}) \\ &\quad - \sin\phi(n, i, j, k)\boldsymbol{b}_{ijk}]\}\end{aligned} \tag{11}$$

where

$$r(i, j) = |\boldsymbol{r}_j - \boldsymbol{r}_i| \tag{12}$$

$$\boldsymbol{b}_{ij} = \frac{\boldsymbol{r}_j - \boldsymbol{r}_i}{r(i, j)} \tag{13}$$

Table 3
$z$-Matrix of the chair conformation of cyclohexane

| Site | $i$ | $r(n, i)$ (Å) | $j$ | $\theta(n, i, j)$ | $k$ | $\phi(n, i, j, k)$ |
|---|---|---|---|---|---|---|
| $C_1$ | | | | | | |
| $C_2$ | 1 | 1.540 | | | | |
| $C_3$ | 2 | 1.540 | 1 | 109.45° | | |
| $C_4$ | 3 | 1.540 | 2 | 109.48° | 1 | 60.02° |
| $C_5$ | 4 | 1.540 | 3 | 109.46° | 2 | −60.03° |
| $C_6$ | 5 | 1.540 | 4 | 109.44° | 3 | 60.00° |

Table 4
Internal cartesian coordinates $x$, $y$, $z$ (in Å) for the six sites of the cyclohexane molecules in the chair conformation, with site $C_1$ located at the origin and the other sites defined by the $z$-matrix given in Table 3 and Eqs. (11)–(16)

| Site | $x$ | $y$ | $z$ |
|---|---|---|---|
| $C_1$ | 0 | 0 | 0 |
| $C_2$ | 1.540 | 0 | 0 |
| $C_3$ | 2.053 | 1.453 | 0 |
| $C_4$ | 1.540 | 2.178 | 1.258 |
| $C_5$ | 0 | 2.178 | 1.258 |
| $C_6$ | −0.513 | 0.726 | 1.258 |

$$\boldsymbol{b}_{ik} = \frac{\boldsymbol{r}_k - \boldsymbol{r}_i}{r(i, k)} \tag{14}$$

$$\theta(k, i, j) = \arccos(\boldsymbol{b}_{ik} \cdot \boldsymbol{b}_{ij}) \tag{15}$$

$$\boldsymbol{b}_{ijk} = \frac{\boldsymbol{b}_{ij} \times \boldsymbol{b}_{ik}}{\sin\theta(k, i, j)} \tag{16}$$

The resulting values of the internal coordinates of the six sites of the cyclohexane molecules in the chair conformation are given in Table 4.

As usual, the site coordinates in the simulation-box frame were computed using the internal coordinates and the rotation matrix [48] based on the three Euler angles $0 \leq \theta \leq 180°$, $-180° \leq \phi \leq 180°$, and $-180° \leq \psi \leq 180°$, as explained in the classic textbook by Allen and Tildesley [44].

The methodology of the REMC method has been described in detail elsewhere [36–38]. A single simulation box is used to simulate single phase reversible reactions. To achieve chemical equilibrium, three kinds of trial moves are performed in the box: molecule translational (and rotational, for benzene and cyclohexane) displacements, box volume changes, and reaction steps. The molecule displacements and the box volume changes are performed in the same way as in the NPT ensemble, with the usual expressions for the probabilities of acceptance of the trial moves [44,49]. For the rotational moves required for benzene and cyclohexane, random orientational displacements were applied following the scheme [44] based on choosing random values for the Euler angles in the rotation matrix, and making use of the internal coordinates of the molecule sites to compute their simulation-box coordinates.

The probability of acceptance for the reaction steps is given by the expression [36]:

$$P_{\mathrm{rx}} = \min\left\{1, V^{\bar{\nu}\xi}\Gamma^{\xi}\exp(-\beta\,\Delta U)\prod_{i=1}^{C}\left[\frac{N_i!}{(N_i + \nu_i\xi)!}\right]\right\} \tag{17}$$

where $V$ is the volume of the box; $C$, the number of species in the reacting system; $\bar{\nu} = \sum_{i=1}^{C}\nu_i$, the change in the total number of molecules per unit of reaction, with $\nu_i$ as the stoichiometric coefficient of species $i$ (positive for the products and negative for the reactants); $\xi$, the extent of reaction; $N_i$, the number of molecules of species $i$ before the reaction step is taken, $\beta = 1/k_B T$ with $k_B$ as Boltzmann's constant and $T$ as absolute temperature, and $\Gamma$ is a function of temperature given by:

$$\Gamma(T) = \left(\frac{P^0}{k_B T}\right)^{\bar{\nu}} \exp\left(\frac{-\Delta G^0_{rx}}{RT}\right) \tag{18}$$

where $\Delta G^0_{rx}$ is the standard Gibbs free energy change of reaction (computed from Eqs. (33) and (38) in Section 4); and $P^0$, the standard pressure.

To perform the reaction steps associated to the hydrogenation of benzene to cyclohexane, first of all, a direction, forward or backward, to take the reaction step, is randomly chosen. If the forward direction is chosen, then $\xi = 1$ and the product in Eq. (17) takes the form:

$$\prod_{i=1}^{C} \frac{N_i!}{(N_i + \nu_i \xi)!} = \frac{N_B N_H (N_H - 1)(N_H - 2)}{N_C + 1} \tag{19}$$

If the backward direction is chosen, then $\xi = -1$ and the product in Eq. (17) takes the form:

$$\prod_{i=1}^{C} \frac{N_i!}{(N_i + \nu_i \xi)!} = \frac{N_C}{(N_B + 1)(N_H + 1)(N_H + 2)(N_H + 3)} \tag{20}$$

For the reaction step in the forward direction, a benzene molecule is randomly picked up, and its potential of interaction with the other molecules is calculated before that molecule is destroyed. Following this, a hydrogen molecule is randomly chosen, and its potential of interaction with the remaining molecules is calculated before that molecule is destroyed. The same procedure is repeated sequentially with two other randomly chosen hydrogen molecules. Finally, a cyclohexane molecule is created in the same position as the benzene molecule that was destroyed, and its potential of interaction with all the surviving molecules is calculated. The total change of energy $\Delta U$ for the reaction step is given by the sum of the five potentials of interaction that were calculated sequentially.

For the reaction step in the backward direction, a sequence consisting of one cyclohexane molecule destruction, and the creation of one benzene molecule (in the same position as the destroyed cyclohexane molecule) and three hydrogen molecules, is performed, so that the total change of energy $\Delta U$ is equal to the sum of the five potentials of interaction sequentially calculated.

Periodic boundary conditions (PBC) and the minimum image convention (MIC), as explained in detail by Allen and Tildesley [44], were applied for the computation of the total configurational energy $U$ or any energy changes $\Delta U$. The MBE6 potentials were not truncated for the computation of the energy and in consequence, long-range corrections were not needed. Simulation runs were initiated with a total number of 864 molecules comprising as many benzene and hydrogen molecules as to comply with the specified value of the hydrogen to benzene feed mole ratio. Starting configurations were generated from previous NPT-ensemble runs for pure benzene at the same temperature and pressure of the reaction. REMC simulation runs required an equilibration phase and a production phase, each consisting of a certain number of cycles, which in turn comprised all three kinds of trial moves. Typically, REMC simulation runs consisted of a total of 5000 cycles with the first 3000 cycles for equilibration and the last 2000 cycles for production. In this way, a sufficiently large number of trial moves were performed during the equilibration phase as to attain stable values of the properties to be sampled in the production phase. A given cycle consisted of translational (and orientational, for benzene and cyclohexane) sequential displacements for all the molecules in the box, followed by one volume change trial move, and as many reaction step trial moves as the total number of benzene and cyclohexane molecules currently present in the box. The formulas for the probabilities of acceptance for the various kinds of moves [36,49] were applied in order to accept or reject a new configuration of the system according to the Metropolis importance sampling technique [44].

In this work, the blocking transformation method developed by Flyvbjerg and Petersen [50], and explained in practical detail by Frenkel and Smit [49], was implemented in order to compute the estimates of the statistical uncertainties (error bars) of the ensemble averages obtained from simulation. Typically, for each fluctuating property, a total of $1.7 \times 10^5$ values were saved to a one-dimensional array during the simulation run. At the end of the run, the entries of this array were collected to define the initial data block on which to apply Flyvbjerg and Petersen's blocking transformation.

## 4. Classical thermodynamics + PSRK method

The chemical equilibrium constant $K_{eq}$ for a gas-phase reaction is given by the expression [51]:

$$K_{eq} = \left(\frac{P}{P^0}\right)^{\bar{\nu}} \prod_{i=1}^{C} (y_i \hat{\varphi}_i)^{\nu_i} \tag{21}$$

where $y_i$ is the mole fraction, $\hat{\varphi}_i$ is the partial fugacity coefficient, and $\nu_i$ is the stoichiometric coefficient (positive for products and negative for reactants) of each of the $C$ species involved in the reaction, $P$ is the pressure of the system, $P^0 = 1\,\text{bar}$ is the standard pressure, and $\bar{\nu} = \sum_i \nu_i$.

The mole fraction $y_i$ at equilibrium is related to the extent of reaction at equilibrium $\xi_{eq}$ by the expression [51]:

$$y_i = \frac{n_{i,0} + \nu_i \xi_{eq}}{n_0 + \nu \xi_{eq}} \tag{22}$$

where $n_{i,0}$ is the number of moles of species $i$ in the feed to the reactor, and $n_0 = \sum_i n_{i,0}$. For the vapor-phase reaction of hydrogenation of benzene to cyclohexane, cyclohexane is not present in the feed to the reactor.

For this reaction, Eq. (21) takes the form:

$$y_C\hat{\varphi}_C - (y_B\hat{\varphi}_B)(y_H\hat{\varphi}_H)^3\left(\frac{P}{P^0}\right)^3 K_{eq} = 0 \tag{23}$$

where the suscripts B, H, and C refer to benzene, hydrogen, and cyclohexane, respectively.

The three partial fugacity coefficients that are required in Eq. (23) can be obtained by application of the PSRK method using the following expression [20]:

$$\begin{aligned}\ln\hat{\varphi}_i &= \frac{B_i}{B_m}(Z_m - 1) - \ln(Z_m - B_m)\\ &\quad - \left\{\frac{A_i}{B_i} + \frac{1}{c^*}\left[\ln\gamma_i + \left(\frac{B_i}{B_m} - 1\right) + \ln\left(\frac{B_m}{B_i}\right)\right]\right\}\\ &\quad \times \ln\left(1 + \frac{B_m}{Z_m}\right)\end{aligned} \tag{24}$$

where $c^* = -0.64663$.

The mixture compressibility factor $Z_m$ is the real root of the SRK cubic equation of state [26]:

$$Z_m^3 - Z_m^2 + (A_m - B_m - B_m^2)Z_m - A_m B_m = 0 \tag{25}$$

which is solved by use of the analytical formulas from the Cardano–Vieta method [52].

The mixing rules of Holderbaum and Gmehling [20] are employed to compute the mixture parameters $B_m$ and $A_m$, as follows:

$$B_m = \sum_i y_i B_i \tag{26}$$

$$A_m = B_m\left\{\sum_i y_i \frac{A_i}{B_i} + \frac{1}{c^*}\left[\frac{G_m^E}{RT} + \sum_i y_i \ln\left(\frac{B_m}{B_i}\right)\right]\right\} \tag{27}$$

where the excess Gibbs free energy of the mixture is obtained from the summability relation for the activity coefficients [51]:

$$\frac{G_m^E}{RT} = \sum_i y_i \ln\gamma_i \tag{28}$$

Table 5
UNIFAC group volume ($R_k$) and surface area ($Q_k$) parameters for the application of the PSRK method to this work (from [20,27])

| Group ($k$) | $R_k$ | $Q_k$ |
|---|---|---|
| $CH_2$ (1) | 0.6744 | 0.540 |
| ACH (3) | 0.5313 | 0.400 |
| $H_2$ (62) | 0.4160 | 0.571 |

The activity coefficients $\gamma_i$ are obtained from the expressions given by Fredenslund et al. [27] for the original UNIFAC group contribution method. Group volume and surface area parameters for $H_2$, and the interaction parameters for $H_2$ with group $CH_2$ (six of which make cyclohexane), and $H_2$ with group ACH (six of which make benzene) have been given by Gmehling and co-workers [20,21]. Group volume and surface area parameters for groups $CH_2$ and ACH, and interaction parameters for group $CH_2$ with group ACH, had already been given by Fredenslund et al. [27] and Skjold-Jørgensen et al. [28], respectively. The group volume ($R_k$) and surface area ($Q_k$) parameters of groups $CH_2$, ACH, and $H_2$ are given in Table 5. The coefficients $a_{mn}$, $b_{mn}$, $c_{mn}$ of the expression

$$\Psi_{mn} = \exp\left(-\frac{a_{mn} + b_{mn}T + c_{mn}T^2}{T}\right) \tag{29}$$

for the temperature dependency of the interaction parameters ($\Psi_{mn}$), are given in Table 6.

The pure component parameters $B_i$ and $A_i$ are given by the expressions [26]:

$$B_i = 0.08664\frac{P_{r,i}}{T_{r,i}} \tag{30}$$

$$A_i = 0.42748\frac{P_{r,i}}{T_{r,i}^2}\alpha(T_{r,i}) \tag{31}$$

where $P_{r,i} = P/P_{c,i}$ and $T_{r,i} = T/T_{c,i}$ with $P_{c,i}$ and $T_{c,i}$ as the critical pressure and temperature of component $i$, respectively, and $\alpha(T_{r,i})$ is the modification by Mathias and Copeman of the SRK alpha function [20]:

$$\begin{aligned}\alpha(T_{r,i}) &= [1 + c_{1,i}(1 - T_{r,i}^{0.5})\\ &\quad + c_{2,i}(1 - T_{r,i}^{0.5})^2 + c_{3,i}(1 - T_{r,i}^{0.5})^3]^2 \quad \text{for } T_{r,i} \le 1\\ \alpha(T_{r,i}) &= [1 + c_{1,i}(1 - T_{r,i}^{0.5})]^2 \quad \text{for } T_{r,i} > 1\end{aligned} \tag{32}$$

Table 6
UNIFAC group interaction parameters for the application of the PSRK method to this work (from [21,28])

| m | n | $a_{mn}$ | $b_{mn}$ | $c_{mn}$ | $a_{nm}$ | $b_{nm}$ | $c_{nm}$ |
|---|---|---|---|---|---|---|---|
| $CH_2$ | ACH | 61.13 | 0 | 0 | −11.12 | 0 | 0 |
| $CH_2$ | $H_2$ | 613.30 | −2.5418 | 0.006638 | 315.96 | −0.4563 | −0.00156 |
| ACH | $H_2$ | 734.87 | 0 | 0 | 16.884 | 0 | 0 |

Table 7
Pure component parameters for the application of the PSRK method to this work (from [20])

| Component | $T_c$ (K) | $P_c$ (bar) | $c_1$ | $c_2$ | $c_3$ |
|---|---|---|---|---|---|
| Benzene | 562.1 | 48.9 | 0.8356 | −0.3750 | 0.9715 |
| Hydrogen | 33.2 | 13.0 | 0.1252 | 0 | 0 |
| Cyclohexane | 553.4 | 40.7 | 0.9031 | −0.8506 | 1.8211 |

Values of the critical temperature $T_c$, critical pressure $P_c$, and the parameters $c_1$, $c_2$, $c_3$ for benzene, hydrogen, and cyclohexane are given in Table 7.

The equilibrium constant $K_{eq}$ is a function only of temperature:

$$K_{eq} = \exp\left(\frac{-\Delta G^0_{rx}}{RT}\right) \tag{33}$$

where $\Delta G^0_{rx}$ is the standard Gibbs free energy change of reaction, and it can be obtained by integration of van't Hoff's equation, as follows [51]:

$$\ln K_{eq} = \int \frac{\Delta H^0_{rx}}{RT^2} dT + J \tag{34}$$

where the standard heat of reaction $\Delta H^0_{rx}$ is in turn obtained from the standard isobaric heat capacity change of reaction:

$$\Delta C^0_{p,rx} = \sum_i \nu_i C^0_{p,i}, \tag{35}$$

by integration of Kirchhoff's equation, as follows [51]:

$$\Delta H^0_{rx} = \int \Delta C^0_{p,rx} dT + I \tag{36}$$

The ideal-gas isobaric heat capacity can be obtained from the following correlation [51]:

$$\frac{C^0_p}{R} = a + bT + cT^2 + dT^{-2} \tag{37}$$

The integration constants $I$ and $J$ are evaluated by application of Eqs. (33)–(37) at a temperature of 298.15 K, where $\Delta H^0_{rx} = \sum_i \nu_i \Delta H^0_{f,i}$ and $\Delta G^0_{rx} = \sum_i \nu_i \Delta G^0_{f,i}$, with $\Delta H^0_f$ and $\Delta \hat{G}^0_f$ as the tabulated values for the standard enthalpy and Gibbs free energy of formation, respectively. When the values given in Table 8 for the standard properties of formation at 298.15 K, and the coefficients $a$, $b$, $c$, $d$ of Eq. (37), are used to perform the integrations indicated in Eqs. (34) and (36), and the integration constants $I$ and $J$ are determined, the following expression for $K_{eq}$ as a function of absolute temperature $T$ (in K) is obtained:

$$\begin{aligned}\ln K_{eq} &= -13.417 \ln T + 1.14595 \times 10^{-2} T - 1.27117 \\ &\quad \times 10^{-6} T^2 - \frac{12450}{T^2} + \frac{2.18189 \times 10^4}{T} + 39.5297\end{aligned} \tag{38}$$

Because the reaction is highly exothermic (with a heat of reaction of 216 kJ/mol at 500 K), the chemical equilibrium constant $K_{eq}$ decreases as temperature is increased. For a given value of reaction temperature $T$, the equilibrium constant $K_{eq}$ is fixed by Eq. (38). If the reaction pressure $P$ is also fixed, then Eq. (23) becomes a non-linear algebraic equation that can be solved for the extent of reaction at equilibrium $\xi_{eq}$ by use of the Newton–Raphson method with the help of Eqs. (24)–(32), and the set of expressions for the combinatorial and residual contributions to the activity coefficients from the UNIFAC method [27].

## 5. Results

### 5.1. Equilibrium conversion

Results for the percentage conversion of benzene to cyclohexane at equilibrium, as a function of pressure, at temperatures of 550, 600, and 650 K, are presented in Figs. 1–4, for hydrogen to benzene (H:B) feed mole ratios of 1.5:1, 3:1, 4.5:1, and 6:1, respectively. To avoid crowded data points, results at 500 K have not been included in Figs. 1–4.

Due to the decrease of the chemical equilibrium constant with temperature caused by the exothermic nature of the reaction, it happens that the conversion of benzene decreases as temperature is increased at fixed values of pressure and H:B feed mole ratio. Since the H:B feed mole ratio of 1.5:1 is below the stoichiometrically required value of 3:1, the conversion of benzene is low with values not exceeding 50%, as shown in Fig. 1. For H:B feed mole ratios of 4.5:1 and 6:1, benzene conversion is 100% at a temperature of 500 K and pressures above 5 bar, and it is also essentially complete at 550 K and pressures above 15 bar, as shown in Figs. 3 and 4.

As expected from the decrease in the total number of moles by reaction, benzene conversion increases with pressure at fixed values of temperature and H:B feed mole ratio. Also, at fixed temperature and pressure, the conversion of benzene increases as the H:B feed mole ratio is increased, as expected from Le Châtelier's principle.

Table 8
Pure component gas-phase standard properties of formation (in kJ/mol) at 298.15 K and coefficients of the heat capacity correlation, Eq. (37) for the calculation of the chemical equilibrium constant of interest to this work (from [51])

| Component | $\Delta H^0_f$ | $\Delta G^0_f$ | $a$ | $b \times 10^3$ | $c \times 10^6$ | $d \times 10^{-5}$ |
|---|---|---|---|---|---|---|
| Benzene | 82.93 | 129.665 | −0.206 | 39.064 | −13.301 | 0 |
| Hydrogen | 0 | 0 | 3.249 | 0.422 | 0 | 0.083 |
| Cyclohexane | −123.14 | 31.92 | −3.876 | 63.249 | −20.928 | 0 |

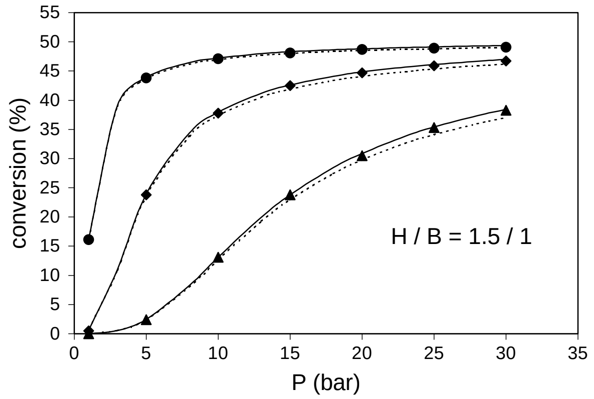

Fig. 1. Percentage conversion of benzene to cyclohexane at equilibrium as a function of pressure and temperature for a hydrogen to benzene (H:B) feed mole ratio of 1.5:1. Filled symbols: REMC molecular simulation (circles for 550 K, diamonds for 600 K, and triangles for 650 K); solid lines: PSRK method; dashed lines: ideal gas assumption.

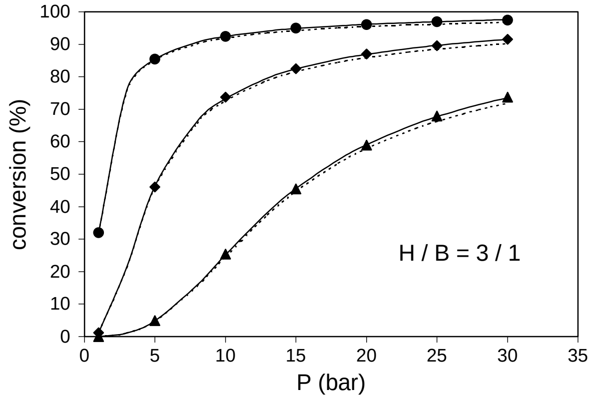

Fig. 2. Percentage conversion of benzene to cyclohexane at equilibrium as a function of pressure and temperature for a hydrogen to benzene (H:B) feed mole ratio of 3:1. Filled symbols: REMC molecular simulation (circles for 550 K, diamonds for 600 K, and triangles for 650 K); solid lines: PSRK method; dashed lines: ideal gas assumption.

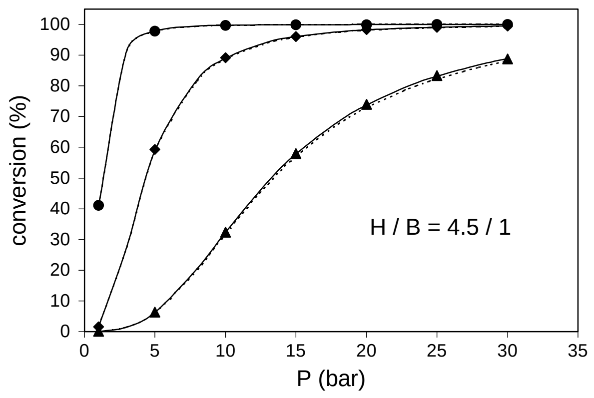

Fig. 3. Percentage conversion of benzene to cyclohexane at equilibrium as a function of pressure and temperature for a hydrogen to benzene (H:B) feed mole ratio of 4.5:1. Filled symbols: REMC molecular simulation (circles for 550 K, diamonds for 600 K, and triangles for 650 K); solid lines: PSRK method; dashed lines: ideal gas assumption.

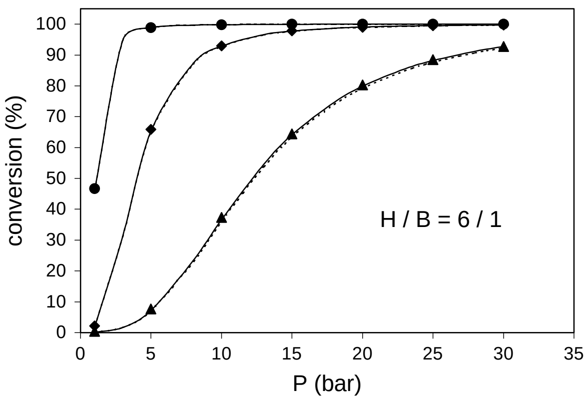

Fig. 4. Percentage conversion of benzene to cyclohexane at equilibrium as a function of pressure and temperature for a hydrogen to benzene (H:B) feed mole ratio of 6:1. Filled symbols: REMC molecular simulation (circles for 550 K, diamonds for 600 K, and triangles for 650 K); solid lines: PSRK method; dashed lines: ideal gas assumption.

As shown in Figs. 1–4, REMC simulation results for the conversion of benzene to cyclohexane are in excellent agreement with results obtained from a combination of classical thermodynamics and the PSRK method. In comparison with the results obtained from the REMC and PSRK methods, the benzene conversion turns out to be slightly underestimated by assuming ideal gas behavior for the three species that take part in the reaction. The deviations shown by the ideal gas results increase at higher temperatures for a fixed value of the H:B feed mole ratio. These deviations are more important at temperatures of 600 and 650 K for the H:B feed mole ratio of 1.5:1; they become less important for the stoichiometric H:B feed mole ratio of 3:1, and they become absolutely negligible at 550 and 600 K for H:B feed mole ratios of 4.5:1 and 6:1.

### 5.2. *Equilibrium composition*

Results for the mole fraction of benzene $y_{\mathrm{B}}$ at equilibrium, as a function of pressure, at temperatures of 550, 600, and 650 K, are presented in Figs. 5–8, for hydrogen to benzene (H:B) feed mole ratios of 1.5:1, 3:1, 4.5:1, and 6:1, respectively. To avoid crowded data points, results at 500 K have not been included in Figs. 5–8.

As expected, these results are entirely consistent with those presented in Figs. 1–4. For the H:B feed mole ratios of 3:1, 4.5:1, and 6:1, hydrogen is either in stoichiometric amount or in excess with respect to benzene. As shown in Figs. 6–8, due to the exothermic nature of the reaction, at fixed values of pressure and H:B feed mole ratio, $y_{\mathrm{B}}$ decreases as temperature is decreased. As expected from the decrease in the total number of moles by reaction, $y_{\mathrm{B}}$ decreases with increasing pressure at fixed values of temperature and H:B feed mole ratio. At fixed conditions of temperature and pressure, $y_{\mathrm{B}}$ decreases as the H:B mole ratio increases, because of the conversion of benzene to cyclohexane and also due to the dilution caused by increasing

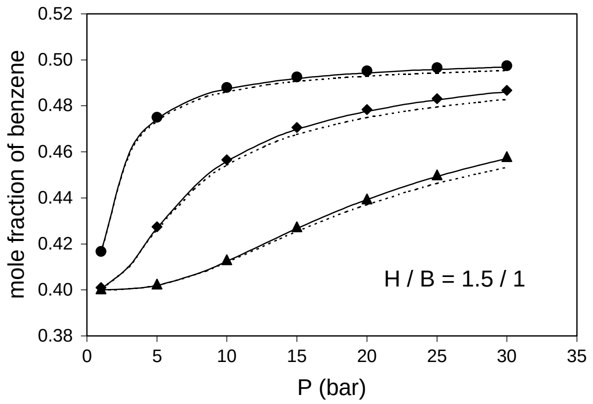

Fig. 5. Mole fraction of benzene at equilibrium as a function of pressure and temperature for a hydrogen to benzene (H:B) feed mole ratio of 1.5:1. Filled symbols: REMC molecular simulation (circles for 550 K, diamonds for 600 K, and triangles for 650 K); solid lines: PSRK method; dashed lines: ideal gas assumption. Error bars for simulation results are much smaller than the size of the symbols.

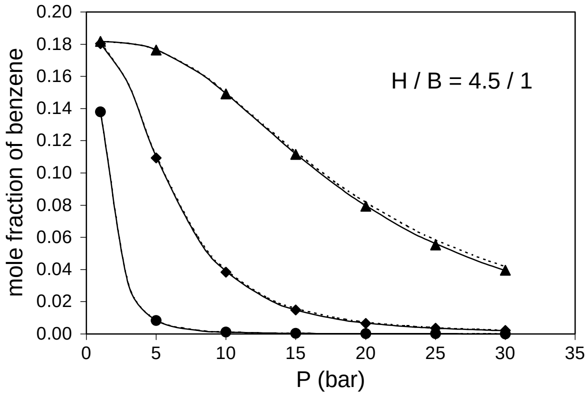

Fig. 7. Mole fraction of benzene at equilibrium as a function of pressure and temperature for a hydrogen to benzene (H:B) feed mole ratio of 4.5:1. Filled symbols: REMC molecular simulation (circles for 550 K, diamonds for 600 K, and triangles for 650 K); solid lines: PSRK method; dashed lines: ideal gas assumption. Error bars for simulation results are much smaller than the size of the symbols.

the amount of hydrogen in the feed to the reactor. In contrast, since hydrogen is the limiting reactant (due to its stoichiometric deficit with respect to benzene) for the H:B feed mole ratio of 1.5:1, an increase in $y_B$ (corresponding to a decrease in the mole fraction of hydrogen) is actually shown in Fig. 5, as temperature is decreased at a given value of pressure.

As shown in Figs. 5–8, REMC simulation results for $y_B$ are in excellent agreement with results obtained from a combination of classical thermodynamics and the PSRK method. As shown in Figs. 6–8, for the H:B feed mole ratios of 3:1, 4.5:1, and 6:1, $y_B$ turns out to be overestimated by assuming ideal gas behavior, in comparison with the results obtained from the REMC and PSRK methods. The deviations shown by the ideal gas results increase at higher temperatures for the higher H:B feed mole ratio values. These deviations become somewhat important at temperatures of 550 and 600 K for the stoichiometric H:B feed mole ratio of 3:1, and they are almost negligible at 550 and 600 K for H:B feed mole ratios of 4.5:1 and 6:1. In contrast, as shown in Fig. 5, for the H:B feed mole ratio of 1.5:1, $y_B$ turns out to be underestimated by assuming ideal gas behavior, in comparison with the results obtained from the REMC and PSRK methods. In this case, the deviations shown by the ideal gas results also increase at higher temperatures and they become certainly important at 650 K.

### 5.3. Equilibrium mixture density

Results for the mass density of the equilibrium mixture, as a function of pressure, at temperatures of 550 and 650 K, are presented in Figs. 9–12, for hydrogen to benzene (H:B)

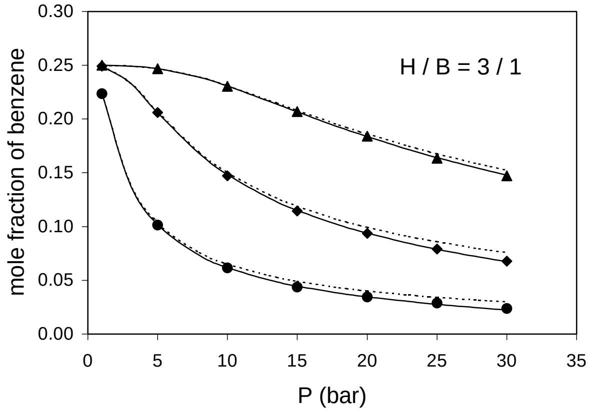

Fig. 6. Mole fraction of benzene at equilibrium as a function of pressure and temperature for a hydrogen to benzene (H:B) feed mole ratio of 3:1. Filled symbols: REMC molecular simulation (circles for 550 K, diamonds for 600 K, and triangles for 650 K); solid lines: PSRK method; dashed lines: ideal gas assumption. Error bars for simulation results are much smaller than the size of the symbols.

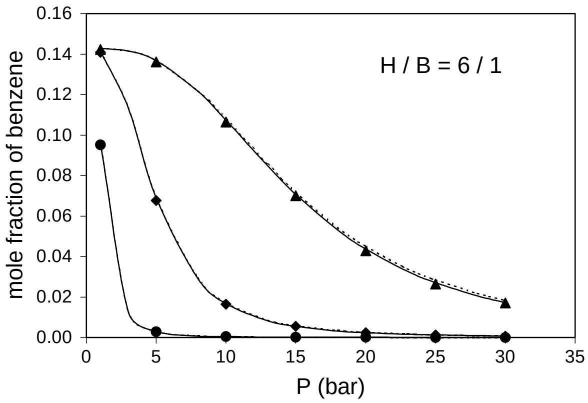

Fig. 8. Mole fraction of benzene at equilibrium as a function of pressure and temperature for a hydrogen to benzene (H:B) feed mole ratio of 6:1. Filled symbols: REMC molecular simulation (circles for 550 K, diamonds for 600 K, and triangles for 650 K); solid lines: PSRK method; dashed lines: ideal gas assumption. Error bars for simulation results are much smaller than the size of the symbols.

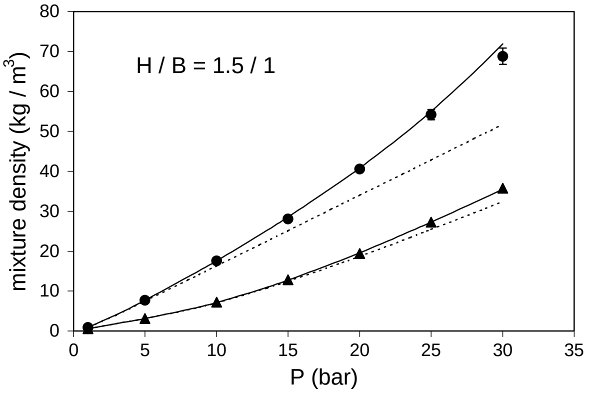

Fig. 9. Mixture mass density at equilibrium as a function of pressure and temperature for a hydrogen to benzene (H:B) feed mole ratio of 1.5:1. Filled symbols: REMC molecular simulation (circles for 550 K, and triangles for 650 K); solid lines: PSRK method; dashed lines: ideal gas assumption. Except for data point at 30 bar and 550 K, error bars for simulation results are much smaller than the size of the symbols.

feed mole ratios of 1.5:1, 3:1, 4.5:1, and 6:1, respectively. To avoid crowded data points, results at 600 K have not been included in Figs. 9–12.

As shown in Figs. 9–12, most of the REMC simulation results for the mass density of the mixture are in excellent agreement with results obtained from a combination of classical thermodynamics and the PSRK method. Some discrepancies occur at 550 K and pressures of 25 and 30 bar, for the H:B feed mole ratios of 1.5:1 and 3:1. In comparison with the results obtained from the REMC and PSRK methods, the mass density of the mixture turns out to be underestimated by assuming ideal gas behavior. The deviations shown by the ideal gas results increase at lower temperatures for a fixed value of the H:B feed mole ratio. These deviations are quite important at a temperature of 550 K for the H:B feed mole ratios of 1.5:1 and 3:1, and they are entirely negligible for a H:B feed mole ratio of 6:1 at 550 and 650 K.

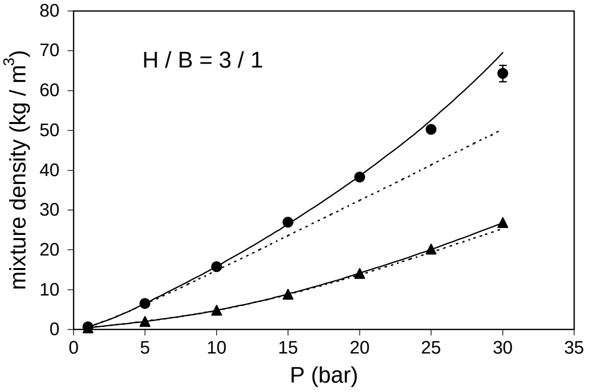

Fig. 10. Mixture mass density at equilibrium as a function of pressure and temperature for a hydrogen to benzene (H:B) feed mole ratio of 3:1. Filled symbols: REMC molecular simulation (circles for 550 K, and triangles for 650 K); solid lines: PSRK method; dashed lines: ideal gas assumption. Except for data point at 30 bar and 550 K, error bars for simulation results are much smaller than the size of the symbols.

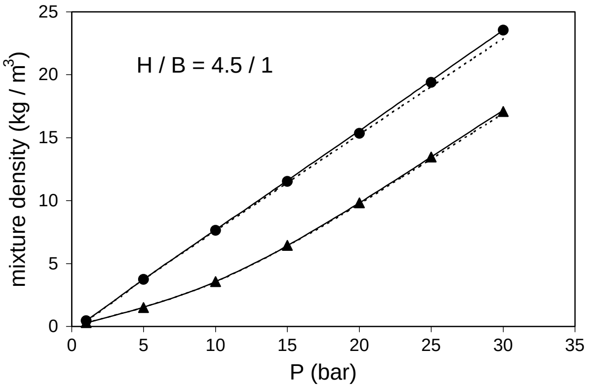

Fig. 11. Mixture mass density at equilibrium as a function of pressure and temperature for a hydrogen to benzene (H:B) feed mole ratio of 4.5:1. Filled symbols: REMC molecular simulation (circles for 550 K, and triangles for 650 K); solid lines: PSRK method; dashed lines: ideal gas assumption. Error bars for simulation results are much smaller than the size of the symbols.

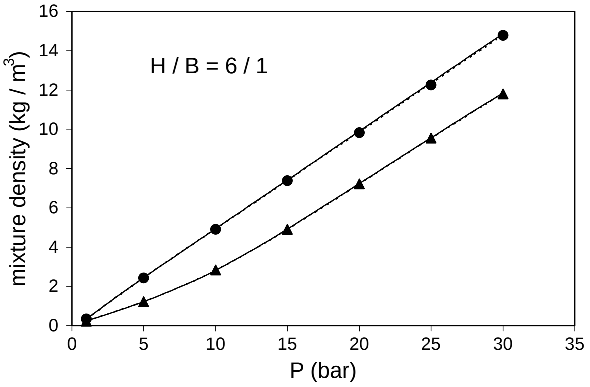

Fig. 12. Mixture mass density at equilibrium as a function of pressure and temperature for a hydrogen to benzene (H:B) feed mole ratio of 6:1. Filled symbols: REMC molecular simulation (circles for 550 K, and triangles for 650 K); solid lines: PSRK method; dashed lines: ideal gas assumption. Error bars for simulation results are much smaller than the size of the symbols.

Interestingly, the significant deviations for the mass density of the equilibrium mixture that are shown by the ideal gas results at 550 K for H:B feed mole ratios of 1.5:1 and 3:1, become less severe for the mole fraction of benzene $y_B$ (Figs. 5 and 6) and become almost insignificant for the benzene conversion (Figs. 1 and 2).

## 6. Conclusions

As expected from a consideration of Le Châtelier's principle, the equilibrium conversion of the exothermic vapor-phase hydrogenation of benzene to cyclohexane increases by either decreasing the temperature, increasing the pressure, or increasing the hydrogen to benzene feed mole ratio.

Due to the lack of experimental chemical equilibrium data for this reaction, it can be said that the excellent agreement between the results obtained in this work from REMC molecular simulation and the PSRK + classical thermodynamics method, is an indirect validation of the predictive capabilities of the effective pair potential models used by Liu and Beck [39] for hydrogen, and developed by Errington and Panagiotopoulos [40] for benzene and cyclohexane.

It turns out from the present work that the assumption of ideal gas behavior for the three species that take part in the reaction, becomes perfectly valid only for a hydrogen to benzene (H:B) feed mole ratio of 6:1 or greater. This result validates the use of the ideal gas assumption made by the authors of a previous study [7] to calculate the benzene concentration in the reactor product at equilibrium, for H:B feed mole ratios of 8:1, 16:1, and 24:1. In contrast, for a H:B feed mole ratio of 3:1 or less, the ideal gas assumption leads to an underestimation of both the benzene conversion and the mixture mass density at equilibrium, the underestimation for the mass density being more severe than that for the conversion. Thus, for a reactor operating with the stoichiometric H:B feed mole ratio of 3:1 (e.g., for the process described in Ref. [17]), use of the PSRK method (instead of the ideal gas assumption) should be made for chemical equilibrium computations because accurate values of the mixture density are important for a reliable and economic design of the tubular reactor.

*List of symbols*

| | |
|---|---|
| $A$ | SRK dimensionless parameter |
| $\boldsymbol{b}$ | intersite separation unit vector |
| $B$ | SRK dimensionless parameter |
| $C$ | number of species in the reacting mixture |
| $C_\mathrm{p}$ | isobaric heat capacity |
| $G$ | Gibbs free energy |
| $H$ | enthalpy |
| $k_\mathrm{B}$ | Boltzmann's constant |
| $K_\mathrm{eq}$ | chemical equilibrium constant |
| $n$ | number of moles |
| $N$ | number of molecules before a reaction step is taken |
| $P$ | pressure |
| $P_\mathrm{rx}$ | probability of acceptance of the reaction step |
| $r$ | intersite separation distance |
| $r(n, i)$ | distance from site $n$ to neighboring site $i$ |
| $r_\mathrm{m}$ | distance at which the original BE6 potential reaches a minimum value |
| $r_\mathrm{max}$ | inner cutoff distance for the MBE6 potential |
| $\boldsymbol{r}$ | intersite separation vector |
| $R$ | gas constant |
| $T$ | absolute temperature |
| $U$ | configurational energy |
| $V$ | simulation box volume |
| $y$ | mole fraction in the vapor phase at equilibrium |
| $Z$ | compressibility factor |

*Greek letters*

| | |
|---|---|
| $\alpha$ | steepness parameter for the MBE6 potential |
| $\alpha(T_\mathrm{r})$ | modified SRK alpha function |
| $\varepsilon$ | energy parameter for the MBE6 potential |
| $\phi$ | pair potential, Euler angle |
| $\phi(n, i, j, k)$ | dihedral angle between the two planes defined by $n$-$i$-$j$ and $i$-$j$-$k$ |
| $\hat{\varphi}$ | partial fugacity coefficient |
| $\gamma$ | activity coefficient |
| $\eta$ | adjustable coefficient for the size parameter combining rule |
| $\nu$ | stoichiometric coefficient |
| $\theta$ | Euler angle |
| $\theta(n, i, j)$ | bond angle at site $i$ between lines $i$–$n$ and $i$–$j$ |
| $\sigma$ | size parameter for the MBE6 potential |
| $\xi$ | extent of reaction |
| $\psi$ | Euler angle |
| $\zeta$ | adjustable coefficient for the energy parameter combining rule |
| $\Delta$ | change |
| $\Gamma$ | temperature dependent function for reaction step |
| $\Psi$ | UNIFAC group interaction parameter |

*Superscripts*

| | |
|---|---|
| E | in excess |
| MBE6 | modified Buckingham exponential-6 |
| 0 | standard state |

*Subscripts*

| | |
|---|---|
| B | for benzene |
| c | critical |
| C | for cyclohexane |
| eq | at equilibrium |
| f | of formation |
| H | for hydrogen |
| $i$ | species index |
| $i, j$ | molecule indices |
| $k, l$ | site indices |
| m | for mixture |
| m, n | UNIFAC group |
| r | reduced |
| rx | reaction |
| 0 | in the reactor feed |

## Acknowledgements

A fellowship for doctoral students from COLCIENCIAS (Instituto Colombiano para el Desarrollo de la Ciencia y la Tecnología Francisco José de Caldas) is gratefully acknowledged by one of the authors (JCM). Financial support from the School of Chemical Engineering, Universidad del Valle, Colombia, is acknowledged by the other author (MLLR).

## References

[1] S. Matar, L.F. Hatch, Chemistry of Petrochemical Processes, Second ed., Butterworth-Heinemann, Boston, 2001, pp. 281–283.
[2] L.F. Hatch, Hydrocarbon Process. 48 (February) (1969) 77–88.
[3] L.F. Hatch, S. Matar, Hydrocarbon Process. 56 (July) (1977) 191–201.
[4] N. Dachos, A. Kelly, D. Felch, E. Reis, in: R.A. Meyers (Ed.), Handbook of Petroleum Refining Processes, Part 4, Second ed., McGraw-Hill, 1997, pp. 4.1–4.26.
[5] R.B. Stobaugh, Hydrocarbon Process. 44 (October) (1965) 157–165.
[6] R.L. Marcell, H.M. Sachs, in: J.J. McKetta, W.A. Cunningham (Eds.), Encyclopedia of Chemical Processing and Design, vol. 14, Marcel Dekker, New York, 1982, pp. 61–82.
[7] O.C. Abraham, G.L. Chapman, Hydrocarbon Process. 70 (October) (1991) 95–97.
[8] L.S. Kassel (assigned to Universal Oil Products Co.), US Patent 2,755,317 (1956).
[9] R. Smith, E.F. Janes (assigned to Texaco Inc.), US Patent 3,254,134 (1966).
[10] R.G. Craig, Chem. Eng. 77 (June 1) (1970) 108–110.
[11] J.C. Hayes (assigned to Universal Oil Products Co.), US Patent 3,700,742 (1972).
[12] J.W. Teter (assigned to Sinclair Refining Co.), US Patent 2,898,387 (1959).
[13] S. Field, M.H. Dalson, Hydrocarbon Process. 46 (May) (1967) 169–174.
[14] Englehard Industries, Hydrocarbon Research, Inc., Sinclair Research, Inc., in: T. Ponder (Ed.), Petrochemical Handbook Issue, Hydrocarbon Process. 46 (November) (1967) p. 163.
[15] F.W. Steffgen (assigned to Atlantic Richfield Co.), US Patent 3,446,863 (1969).
[16] Atlantic Richfield Co. in: T. Ponder (Ed.), Petrochemical Handbook Issue, Hydrocarbon Process. 52 (November) (1973) p. 116.
[17] Arco Technology, Inc. in: T. Ponder (Ed.), Petrochemical Handbook Issue, Hydrocarbon Process. 56 (November) (1977) p. 143.
[18] A.M. Jose (assigned to YPF S.A.), US Patent 6,153,805 (2000).
[19] Chemstations, Inc., Houston. CHEMCAD Version 5.3, Help/Thermodynamics/K-value models/K-value special components/Hydrogen.
[20] T. Holderbaum, J. Gmehling, Fluid Phase Equilib. 70 (1991) 251–265.
[21] K. Fischer, J. Gmehling, Fluid Phase Equilib. 121 (1996) 185–206.
[22] J. Gmehling, J. Li, K. Fischer, Fluid Phase Equilib. 141 (1997) 113–127.
[23] J. Li, K. Fischer, J. Gmehling, Fluid Phase Equilib. 143 (1998) 71–82.
[24] S. Hortsmann, K. Fischer, J. Gmehling, Fluid Phase Equilib. 167 (2000) 173–186.
[25] J. Chen, K. Fischer, J. Gmehling, Fluid Phase Equilib. 200 (2002) 411–429.
[26] G. Soave, Chem. Eng. Sci. 27 (1972) 1197–1203.
[27] A. Fredenslund, R.L. Jones, J.M. Prausnitz, AIChE J. 21 (1975) 1086–1099.
[28] S. Skjold-Jørgensen, B. Kolbe, J. Gmehling, P. Rasmussen, Ind. Eng. Chem. Proc. Des. Dev. 18 (1979) 714–722.
[29] J. Gmehling, P. Rasmussen, A. Fredenslund, Ind. Eng. Chem. Proc. Des. Dev. 21 (1982) 118–127.
[30] E.A. Macedo, U. Weidlich, J. Gmehling, P. Rasmussen, Ind. Eng. Chem. Proc. Des. Dev. 22 (1983) 676–678.
[31] D. Tiegs, J. Gmehling, P. Rasmussen, A. Fredenslund, Ind. Eng. Chem. Res. 26 (1987) 159–161.
[32] H.K. Hansen, P. Rasmussen, A. Fredenslund, M. Schiller, J. Gmehling, Ind. Eng. Chem. Res. 30 (1991) 2352–2355.
[33] J.J. Potoff, J.I. Siepmann, AIChE J. 47 (2001) 1676–1682.
[34] J. Carrero-Mantilla, M. Llano-Restrepo, Fluid Phase Equilib. 208 (2003) 155–169.
[35] J. Carrero-Mantilla, M. Llano-Restrepo, Mol. Simul. 29 (2003) 549–554.
[36] W.R. Smith, B. Triska, J. Chem. Phys. 100 (1994) 3019–3027.
[37] M. Lisal, I. Nezbeda, W.R. Smith, J. Chem. Phys. 110 (1999) 8597–8604.
[38] M. Lisal, W.R. Smith, I. Nezbeda, AIChE J. 46 (2000) 866–875.
[39] A. Liu, T.L. Beck, J. Chem. Phys. 105 (1996) 2424–2428.
[40] J.R. Errington, A.Z. Panagiotopoulos, J. Chem. Phys. 111 (1999) 9731–9738.
[41] P.T. Cummings, B.K. Peterson, C.K. Hall, M. Neurock, A.Z. Panagiotopoulos, P.R. Westmoreland, Final Report of the Workshop Future Directions in Molecular Modeling and Simulation: Fundamentals and Applications, National Science Foundation, Arlington, November 1997.
[42] J.O. Hirschfelder, C.F. Curtiss, R.B. Bird, Molecular Theory of Gases and Liquids, Wiley, New York, 1954, pp. 33–34.
[43] T.M. Reed, K.E. Gubbins, Applied Statistical Mechanics, McGraw-Hill, New York, 1973, pp. 110–112.
[44] M.P. Allen, D.J. Tildesley, Computer Simulation of Liquids, Clarendon Press, Oxford, 1987.
[45] R.T. Morrison, R.N. Boyd, Organic Chemistry, Fifth ed., Allyn & Bacon, Boston, 1987 (Chapter 12), Section 12.11.
[46] F. Jensen, Introduction to Computational Chemistry, Wiley, New York, 1999, pp. 414–421.
[47] H. Essén, M. Svensson, Comput. Chem. 20 (1996) 389–395.
[48] H. Goldstein, Classical Mechanics, second ed., Addison-Wesley, Reading, 1980, pp. 143–148.
[49] D. Frenkel, B. Smit, Understanding Molecular Simulation, From Algorithms to Applications, Academic Press, San Diego, 1996.
[50] H. Flyvbjerg, H.G. Petersen, J. Chem. Phys. 91 (1989) 461–466.
[51] J.M. Smith, H.C. Van Ness, M.M. Abbott, Introduction to Chemical Engineering Thermodynamics, fifth ed., McGraw-Hill, New York, 1996.
[52] W.H. Press, B.P. Flannery, S.A. Teukolsky, W.T. Vetterling, Numerical Recipes: The Art of Scientific Computing (FORTRAN Version), Cambridge University Press, Cambridge, 1989, p. 146.